Semi-Lagrangian Integration of a Gridpoint Shallow Water Model on the Sphere

A. MCDONALD AND J. R. BATES*

Irish Meteorological Service, Dublin

(Manuscript received 5 April 1988, in final form 19 July 1988)

ABSTRACT

A stable, semi-Lagrangian, semi-implicit, two-time-level, gridpoint integration scheme for the shallow water equations on the sphere is presented. A rotated spherical coordinate system is used to integrate the equations of motion at each gridpoint poleward of a certain latitude, thus overcoming problems associated with the polar singularity. The results of medium term integrations of large scale test patterns using a long time step are presented.

1. Introduction

The semi-Lagrangian approach to integrating NWP models has been undergoing considerable development during the past few years. This approach allows the use of long advective time steps and, when combined with stable methods for treating the adjustment process, offers the advantage of greatly increased efficiency of integration compared with Eulerian schemes in which advection is treated explicitly.

Most of the work on semi-Lagrangian schemes has been carried out in the context of limited-area gridpoint models, using the geometrical framework of either a polar stereographic projection (Robert 1981, 1982; Robert et al. 1985) or a rotated latitude–longitude grid whose pole is well removed from the area of interest (Bates and McDonald 1982, 1987; Bates 1984; McDonald 1986). Staniforth and Temperton (1986) and Temperton and Staniforth (1987) have developed limited area finite element models, their geometry being based on a polar stereographic projection.

There is a natural interest in extending semi-Lagrangian schemes to the global domain. One of the problems associated with limited-area models—that particles sometimes originate outside the region of integration—no longer occurs when a model becomes global. It is therefore possible that semi-Lagrangian schemes will only achieve their full potential in the global context. Before this can occur, however, the problems associated with the polar singularity in the latitude–longitude coordinate system must be solved. From the point of view of semi-Lagrangian integration, these are the following:

(i) The departure point corresponding to a near-polar grid point cannot be accurately located by going back along the coordinate lines using the known velocity components at a single point, because of the strong curvature of the coordinate lines near the singularity.

(ii) The momentum equations in component form cannot be accurately integrated along a near-polar trajectory corresponding to a long time step, because of the rapid spatial variation of all terms in the equations (particularly the curvature terms) along such a trajectory.

Recently, Ritchie (1988) has developed a global three-time-level spectral shallow water model in which problem (i) is solved by using an associated Cartesian coordinate system whose origin is at the center of the earth, while problem (ii) is solved by integrating the momentum equation in vector form. Coté and Staniforth (1988) have developed a global two-time-level spectral shallow water model in which problem (ii) is solved by using a great circle approach, while the momentum equation is again treated in a vector manner.

In the present paper we are concerned with a gridpoint method of integrating the shallow water equations. We solve both of the pole problems by using an auxiliary spherical coordinate system at each gridpoint poleward of a certain latitude (for the pole itself, a separate procedure is used). The auxiliary system is obtained by a rotation such that the new equator passes through the gridpoint in question and the new coordinate directions coincide with those of the original system at that point. The departure point can be accurately located and the momentum equations accurately integrated in the auxiliary system, because of the minimal curvature of the new coordinate lines near

* Present affiliation: NASA/Goddard Laboratory for Atmospheres and University of Maryland

Corresponding author address: Dr. J. R. Bates, NASA/Goddard Space Flight Center, Code 611, Building 22, Greenbelt, MD 20771.

the point of interest. A transformation back to the original system (involving interpolations to the departure point from surrounding gridpoints in that system) completes the procedure.

The proposed method is applied to the shallow water equations on the sphere and integrations are successfully carried out for a situation involving strong cross-polar flow. The particular integration scheme we use derives from the two-time-level, semi-Lagrangian and semi-implicit scheme on a C-grid developed by McDonald (1986).

2. Integration of the shallow water equations

A semi-Lagrangian scheme for integrating an equation of the form

$$\frac{d_H\Psi}{dt} = \xi \tag{1}$$

where $(d/dt)_H$ is the horizontal Lagrangian derivative will be based upon some approximation to the formula

$$\Psi^{n+1} - \Psi^n_* = \int_{n\Delta t}^{(n+1)\Delta t} \xi dt \tag{2}$$

where Ψ^{n+1} is the value of Ψ at an arrival point at the new time level, Ψ^n_* is its value at the corresponding departure point at the old time level (asterisk subscripts will always denote values at departure points in what follows), and the rhs represents an integral along the trajectory over the time interval Δt. The simplest method of locating the departure point is to go back from the arrival point along the coordinate lines using the formulae

$$\lambda_* = \lambda - \left(\frac{\hat{u}}{a\cos\hat{\theta}}\right)\Delta t \tag{3}$$

$$\theta_* = \theta - \left(\frac{\hat{v}}{a}\right)\Delta t \tag{4}$$

where $\hat{}$ denotes a space and time centered estimate along the trajectory (see McDonald and Bates 1987). In the neighborhood of the polar singularity, Eqs. (3) and (4) will no longer provide accurate estimates of the position of the departure point. Furthermore, if ξ varies rapidly along the trajectory (as do the components of the velocity, the components of the gradient operator and the curvature terms near the pole), the rhs of (2) cannot be accurately estimated using any simple numerical formula such as $(\xi^{n+1} + \xi^n_*)\Delta t/2$. For these reasons it is appropriate in considering the integration of the equations of motion to deal separately with regions removed from and in the neighborhood of the poles.

In what follows we are concerned specifically with the integration of the shallow water equations, with divergence damping included. Our equations are

$$\frac{d_H u}{dt} = -\frac{1}{a\cos\theta}\frac{\partial}{\partial\lambda}(\phi - cD) + fv + C_u \tag{5}$$

$$\frac{d_H v}{dt} = -\frac{1}{a}\frac{\partial}{\partial\theta}(\phi - cD) - fu + C_v \tag{6}$$

$$\frac{d_H \phi}{dt} = -\phi D \tag{7}$$

where D is the divergence given by

$$D = \frac{1}{a\cos\theta}\left[\frac{\partial u}{\partial\lambda} + \frac{\partial}{\partial\theta}(v\cos\theta)\right].$$

Here c is the coefficient of divergence damping, C_u, C_v are the curvature terms, given by

$$C_u = \frac{uv\tan\theta}{a}, \quad C_v = -\frac{u^2\tan\theta}{a}$$

and the remaining notation is conventional. Note that the curvature terms can easily exceed the Coriolis terms in magnitude near the poles.

a. *Region removed from the poles ($|\theta| \leq \theta_M$)*

Following the procedure used by McDonald (1986), we integrate the momentum equations (5) and (6) in two half time-steps of $\Delta t/2$. In the first half-step the Coriolis terms are treated implicitly while the pressure gradient and divergence damping terms are treated explicitly; in the second half-step the converse is the case. The curvature terms are integrated for a full Δt in the first step. Thus we have

Step 1:

$$(u^{n+1/2} - u^n_*)/(\Delta t/2) = \left[-\frac{1}{a\cos\theta}\frac{\partial}{\partial\lambda}(\phi - cD) + 2C_u\right]^n_* + f_* v^{n+1/2} \tag{8}$$

$$(v^{n+1/2} - v^n_*)/(\Delta t/2) = \left[-\frac{1}{a}\frac{\partial}{\partial\theta}(\phi - cD) + 2C_v\right]^n_* - f_* u^{n+1/2}. \tag{9}$$

Step 2:

$$(u^{n+1} - u^{n+1/2})/(\Delta t/2) = -\left[\frac{1}{a\cos\theta}\frac{\partial}{\partial\lambda}(\phi - cD)\right]^{n+1} + fv^{n+1/2} \tag{10}$$

$$(v^{n+1} - v^{n+1/2})/(\Delta t/2) = -\left[\frac{1}{a}\frac{\partial}{\partial\theta}(\phi - cD)\right]^{n+1} - fu^{n+1/2}. \tag{11}$$

The continuity equation (7) is integrated in a single step of Δt as follows:

$$(\phi^{n+1} - \phi^n_*)/\Delta t = -(\bar{\phi}/2)(D^{n+1} + D^n_*) - (\phi' D)^n_*. \tag{12}$$

In the above, $\bar{\phi}$ is a constant such that $\phi = \bar{\phi} + \phi'$, $|\phi'| \ll \bar{\phi}$. Variables without subscripts denote values at arrival points while variables with an asterisk subscript denote values at the corresponding departure points, these points being located using (3), (4). Note that no spatial discretization has yet been introduced.

We solve (8), (9) for $(u, v)^{n+1/2}$ and eliminate these quantities from (10), (11). Bringing all $(n+1)$-level quantities to the left in the resulting equations and treating (12) in like manner we have

$$\left[u + \frac{\Delta t}{2}\frac{1}{a\cos\theta}\frac{\partial}{\partial\lambda}(\phi - cD)\right]^{n+1} = B_u \quad (13)$$

$$\left[v + \frac{\Delta t}{2}\frac{1}{a}\frac{\partial}{\partial\theta}(\phi - cD)\right]^{n+1} = B_v \quad (14)$$

$$\left[\phi + \frac{\Delta t}{2}\bar{\phi}D\right]^{n+1} = B_\phi \quad (15)$$

where

$$B_u = (W_u)^n_* + F(W_v)^n_*$$

$$B_v = (W_v)^n_* - F(W_u)^n_*$$

$$B_\phi = \left[\phi - \left(\frac{\Delta t}{2}\bar{\phi} + \Delta t\phi'\right)D\right]^n_*$$

with

$$W_u = \frac{Y_u + F\bar{Y}_v}{1 + F^2}$$

$$W_v = \frac{Y_v - F\bar{Y}_u}{1 + F^2}$$

$$Y_u = u - \frac{\Delta t}{2}\frac{1}{a\cos\theta}\frac{\partial}{\partial\lambda}(\phi - cD) + \Delta t C_u$$

$$Y_v = v - \frac{\Delta t}{2}\frac{1}{a}\frac{\partial}{\partial\theta}(\phi - cD) + \Delta t C_v$$

$$F = f\Delta t/2.$$

Our spatial discretization is based on a C-grid (see Fig. 1). The quantities (B_u, B_v, B_ϕ) are expressed at (u, v, ϕ) points, respectively. The asterisk subscripts that occur in the definition of these quantities thus denote quantities evaluated at the departure points of trajectories which arrive at u, v or ϕ points, as appropriate. The overbars occurring in the definition of (W_u, W_v) denote 16-point averages evaluated at (u, v) points, respectively. From (13) and (14) we find

$$D^{n+1} = \nabla\cdot\mathbf{B} - \frac{\Delta t}{2}\nabla^2(\phi - cD)^{n+1} \quad (16)$$

where $\mathbf{B} = (B_u, B_v)$. Eliminating D^{n+1} between (15) and (16) gives the Helmholtz equation

$$\nabla^2\phi^{n+1} - \mu^2\phi^{n+1} = H \quad (17)$$

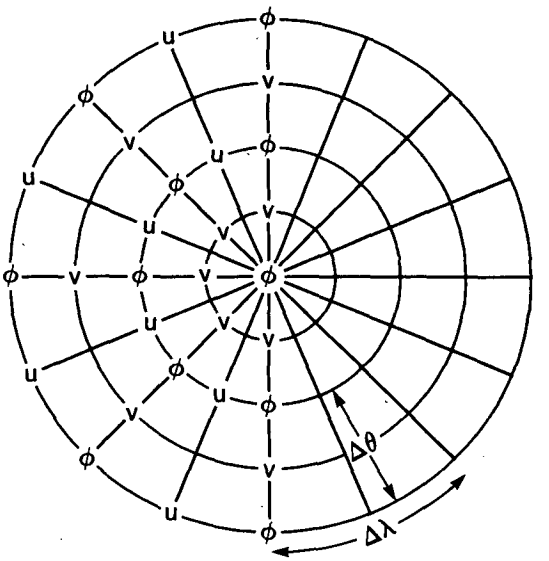

FIG. 1. The distribution of variables on the C-grid in the neighborhood of the pole.

where

$$\mu^2 = \left[\left(\frac{\Delta t}{2}\right)^2\bar{\phi} + c\frac{\Delta t}{2}\right]^{-1}$$

$$H = \mu^2\left[\left(\frac{\Delta t}{2}\bar{\phi}\right)\nabla\cdot\mathbf{B} + \left(c\frac{\Delta t}{2}\nabla^2 - 1\right)B_\phi\right].$$

The Helmholtz equation (17) is solved using the fast solver of Sweet (1977). Once ϕ^{n+1} is known, $(D, u, v)^{n+1}$ are determined from (15), (13), (14).

The reason for integrating the momentum equations in two half steps is simply to generate an equation of the form (17) for which a fast solver exists. The system of equations is not split in the conventional sense, since no $(n+1/2)$-level quantities are actually computed: Eqs. (13), (14), (15) contain only quantities at time levels n and $(n+1)$.

b. *Neighborhood of a pole ($|\theta| > \theta_M$)*

In the neighborhood of a pole ($|\theta| > \theta_M$) we continue to integrate our equations using the gridpoints of the original (λ, θ) C-grid. However, for the purposes of accurately locating the departure points and of integrating the momentum equations in a system in which their terms are smoothly varying, we introduce for each near-polar gridpoint A (at which $\lambda = \lambda_I$, $\theta = \theta_J$) an auxiliary spherical coordinate system (λ', θ') such that in the new system the point A lies at $(\lambda' = 0, \theta' = 0)$ and the coordinate unit vectors $(\mathbf{i}, \mathbf{j})$ at point A in both systems coincide (see Fig. 2).

The coordinates of an arbitrary point in the auxiliary and the original coordinate systems are related by the following formulae (see appendix A):

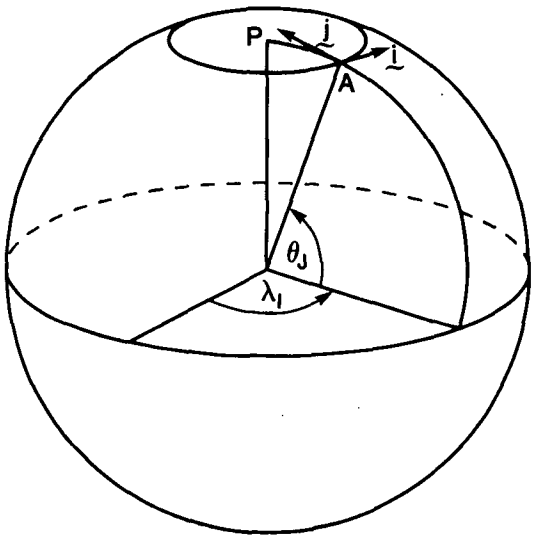

FIG. 2. The auxiliary coordinate system at point A is obtained by rotating the geographical spherical system through the angles λ_I and θ_J.

$$\cos\theta' \cos\lambda' = \cos\theta \cos(\lambda - \lambda_I) \cos\theta_J + \sin\theta \sin\theta_J \tag{19}$$

$$\cos\theta' \sin\lambda' = \cos\theta \sin(\lambda - \lambda_I) \tag{20}$$

$$\sin\theta' = \sin\theta \cos\theta_J - \cos\theta \cos(\lambda - \lambda_I) \sin\theta_J \tag{21}$$

from which the inverse formulae

$$\lambda = \lambda_I + \tan^{-1}\left[\frac{\cos\theta' \sin\lambda'}{\cos\theta' \cos\lambda' \cos\theta_J - \sin\theta' \sin\theta_J}\right] \tag{22}$$

$$\theta = \sin^{-1}[\cos\theta' \cos\lambda' \sin\theta_J + \sin\theta' \cos\theta_J] \tag{23}$$

are obtained.

Using (19)–(21) it can be shown (see appendix A) that the velocity components in the two systems are related by

$$\begin{pmatrix} u' \\ v' \end{pmatrix} = \begin{pmatrix} \mathcal{G}, & -\mathcal{S} \\ \mathcal{S}, & \mathcal{G} \end{pmatrix} \begin{pmatrix} u \\ v \end{pmatrix} \tag{24}$$

where

$$\mathcal{G} = [\cos\theta \cos\theta_J + \sin\theta \sin\theta_J \cos(\lambda - \lambda_I)]/\cos\theta'$$

$$\mathcal{S} = \sin\theta_J \sin(\lambda - \lambda_I)/\cos\theta'.$$

Note that at the point A, $\mathcal{G} = 1$, $\mathcal{S} = 0$.

It can be shown that the components of $\nabla\phi$ transform in the same manner as the velocity components.

Due to the small curvature of the coordinate lines in the auxiliary system in the neighborhood of the point A, the departure point corresponding to point A can be accurately located using the formulae

$$\lambda'_* = -\left(\frac{\hat{u}'}{a \cos\hat{\theta}'}\right)\Delta t \tag{25}$$

$$\theta'_* = -\left(\frac{\hat{v}'}{a}\right)\Delta t \tag{26}$$

whence its coordinates in the original system are obtained using the inverse formulae (22) and (23). The space centering used to obtain $(\hat{u}', \hat{v}')$ in (25) and (26) consists of an iterative procedure. The first estimate is to set $(\hat{u}', \hat{v}')$ equal to $(u', v')_A$ which, by (24), are identical to the known quantities $(u, v)_A$. Successive estimates are obtained as follows: (i) Replace Δt by $\Delta t/2$ in (25), (26) to obtain the coordinates of the midpoint M of the trajectory in the auxiliary system; (ii) Transform back to obtain the coordinates of M in the original system using (22), (23); (iii) Interpolate velocity components to M from surrounding gridpoints in the original system, giving $(u, v)_M$; (d) Convert $(u, v)_M$ to $(u', v')_M$ using (24) and take the result as the latest estimate of $(\hat{u}', \hat{v}')$.

We also need to determine the departure points corresponding to the poles themselves, since ϕ is a prognostic variable at the poles. The method used for doing this is described in appendix B.

We now integrate the momentum equations in the auxiliary coordinate system using the two-step method described earlier. This leads to equations of the same form as [(8), (9), (10), (11)] in the transformed coordinates. We use the simplification of omitting the curvature terms in the transformed system; that these are small can be seen from the fact that

$$\left|\frac{C'_u}{fv'}\right| = \left|\frac{C'_v}{fu'}\right| = \left(\frac{u'}{2\Omega a}\right)\left(\frac{\tan\theta'}{\sin\theta}\right) \ll 1 \quad \text{for} \quad |\theta'| \ll 1.$$

Using (24) to transform the components of the velocity and $\nabla\phi$ at the arrival and departure points back to the original system, our equations corresponding to (13), (14) then become

$$\left[u + \frac{\Delta t}{2}\frac{1}{a\cos\theta}\frac{\partial}{\partial\lambda}(\phi - cD)\right]^{n+1} = A_u \tag{27}$$

$$\left[v + \frac{\Delta t}{2}\frac{1}{a}\frac{\partial}{\partial\theta}(\phi - cD)\right]^{n+1} = A_v \tag{28}$$

where

$$A_u = (\mathcal{G}_* + F\mathcal{S}_*)(W_u)^n_* - (\mathcal{S}_* - F\mathcal{G}_*)(W_v)^n_*$$

$$A_v = (\mathcal{G}_* + F\mathcal{S}_*)(W_v)^n_* + (\mathcal{S}_* - F\mathcal{G}_*)(W_u)^n_*.$$

Here the (W_u, W_v) are as previously defined except that the curvature terms are omitted.

The continuity equation (15), which involves only scalars, maintains the same form in the neighborhood of the poles as elsewhere; it requires the use of the auxiliary coordinate system only to determine the departure point at which the rhs is evaluated. Equations (15), (27) and (28) again reduce to a Helmholtz equation of the form (17), the only difference being that the forcing function on the rhs is now given by

$$H = \mu^2\left[\left(\frac{\Delta t}{2}\bar{\phi}\right)\nabla\cdot\mathbf{A} + \left(c\frac{\Delta t}{2}\nabla^2 - 1\right)B_\phi\right] \quad (29)$$

where $\mathbf{A} = (A_u, A_v)$. Thus, our auxiliary coordinate system has allowed an extension of the Helmholtz equation to the whole sphere, while overcoming the problems associated with the polar singularity.

In all our numerical computations we used bicubic interpolation to obtain values at departure points, while using bilinear interpolation to obtain values at the midpoints of trajectories for the purpose of space centering. In the case of points lying in the immediate neighborhood of the poles, the interpolations used values at gridpoints lying on the other side of the poles. Whenever vector components from across the poles were used, they underwent a change of sign. All divergences at the poles were evaluated using the integral rather than the differential definition.

3. Numerical results

Numerical integrations were carried out to test the above scheme on the global domain. As initial state we chose a geopotential field given by

$$\phi(\lambda, \theta, 0) = \bar{\phi} + 2\Omega a v_0 \sin^3\theta\cos\theta\sin\lambda \quad (30)$$

where Ω and a are, respectively, the earth's rotation rate and radius. The initial wind field was derived from (30) using the geostrophic relationship. Thus, the initial cross-polar flow was of strength v_0, while both wind components were zero at the equator. The values $\bar{\phi} = 5.768 \times 10^4\ \mathrm{m^2\ s^{-2}}$ and $v_0 = 20\ \mathrm{m\ s^{-1}}$ were used in the integrations. The initial fields are displayed in Fig. 3.

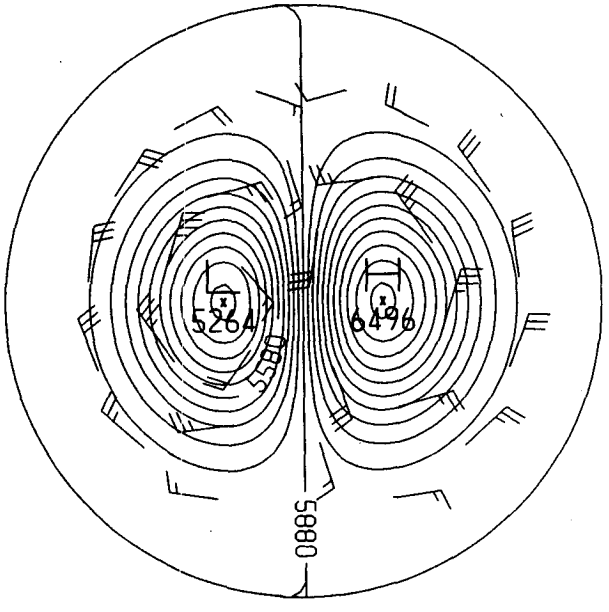

FIG. 3. Initial fields (geopotential height in meters, with contour interval = 60 m; wind speed in knots).

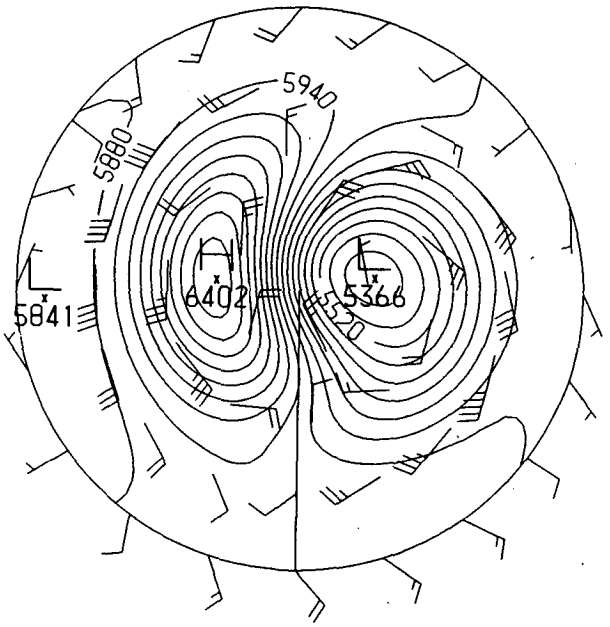

FIG. 4. Reference integration at day 5 ($\Delta\lambda = \Delta\theta = 3°$, $\theta_M = 60°$, $c = 6.8 \times 10^6\ \mathrm{m^2\ s^{-1}}$, $\Delta t = 10$ min).

As the basic set of parameter values we chose $\Delta\lambda = \Delta\theta = 3°$, $\theta_M = 60°$, $c = 6.8 \times 10^6\ \mathrm{m^2\ s^{-1}}$. The model was first integrated with a small time step of $\Delta t = 10$ min to provide a reference forecast. The trajectories were calculated using the space and time-centering scheme of McDonald and Bates (1987), with one iteration to achieve space centering. The results of the 5-day reference integration are shown in Fig. 4. It can be seen that the dynamical fields are noise-free. It was found, however, that the smoothness of the integration depended essentially on the presence of the divergence damping. With $c = 0$ the fields were very noisy even at day 1, though the integration was still stable at day 10. The noise problem was not alleviated by decreasing θ_M from 60° to 45°.

We next increased the time step to $\Delta t = 1$ h, with all other parameters as in the reference run. The results of the 5-day integration for this case are shown in Fig. 5. It can be seen that the results are very close to those of the reference run. The rms height difference from the reference run at day 5 amounts to 9.8 m. This indicates an acceptable level of accuracy (an rms error of 3 m day^{-1} has been adopted by the Canadian workers in this field as the criterion of acceptability; see Coté and Staniforth 1988).

Unlike the case with the short time step, it was found that divergence damping was not necessary to maintain a smooth integration with the longer time step. The result of a 5-day integration with $\Delta t = 1$ h and $c = 0$ are shown in Fig. 6. The rms difference from the references run was again 9.8 m.

For time steps longer than 1 h, the rms height differences from the reference run began to increase ap-

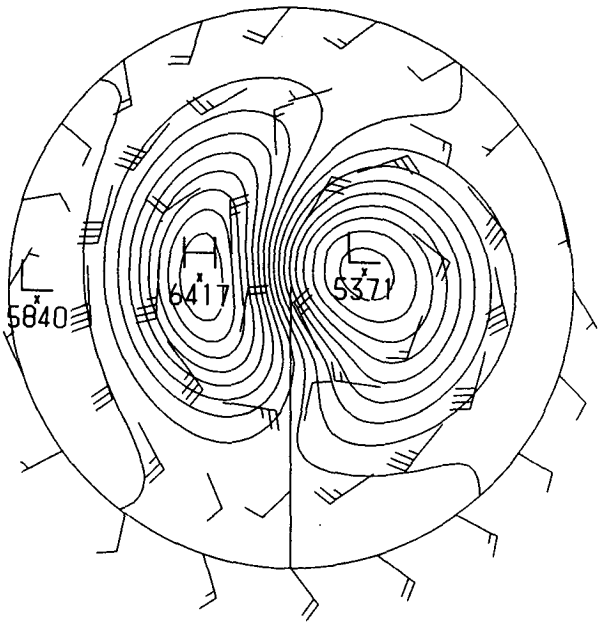

FIG. 5. Integration at day 5 with Δt = 1 h (remaining parameters as in Fig. 4).

preciably. We were unable to match the results of Coté and Staniforth (1988), who achieved an acceptable accuracy with their two-time-level spectral model using time steps as large as 2 h (see their Fig. 6). Presumably, the main reason we were unable to do this is because of the error introduced by our two-step method of integrating the momentum equations. The accuracy of our integrations was also limited by the fact that, unlike Coté and Staniforth, we did not have a normal mode initialization scheme at our disposal to balance the initial state; gravity waves of appreciable amplitude were present in our integrations for up to 2 days. It has been shown by H. Ritchie (personal communication) that the presence of gravity waves can contribute appreciably to the error of a semi-Lagrangian integration.

The integration scheme presented here does not formally conserve any of the quantities which are conserved by the analytical shallow water equations. Nevertheless, its conservation properties were generally found to be quite good. For a forecast starting from the geostrophically balanced initial state shown in Fig. 3, with Δt = 1.5 h, c = 0, θ_M = 60°, and with space and time-centering of the trajectories (one iteration), the mass, total energy and potential enstrophy after 10 days were, respectively, 1.0004, 1.0009 and 0.9931 times their initial values. When the integrations were continued out to 30 days, it was found necessary to use divergence damping with $c = 6.8 \times 10^6$ m^2 s^{-1} in order to maintain these properties. At 30 days, the mass, energy and potential enstrophy were then found to be 1.001, 1.003, and 0.980 times their initial values.

In order to see whether the above results depend on the initial state, we carried out an integration starting from a different initial field. This consisted of the gravest symmetrical rotational Hough mode of zonal wavenumber 1, with a mean height of 10 km and a perturbation amplitude of 1 km. The model parameters were chosen to be $\Delta\lambda = \Delta\theta = 3°$, $c = 6.8 \times 10^6$ m^2 s^{-1}, Δt = 1.5 h, and $\theta_M = 45°$ ($\theta_M = 60°$ gave rise to noise in the region of the pole). The relative values of mass, energy and potential enstrophy after 10 days were 1.0005, 1.0014 and 0.9935. However, from day 20 onwards these quantities ceased to be almost conserved, so that by day 30 their relative values were 0.96, 0.92 and 1.08. Increasing the divergence damping coefficient to 1.1×10^7 m^2 s^{-1} restored the integration to its "almost conserving" mode, yielding at 30 days the relative values of 1.0018, 1.0051 and 0.9811 for mass, energy and potential enstrophy.

4. Conclusions

A gridpoint shallow water model has been integrated on the sphere using a semi-Lagrangian, semi-implicit, two-time-level integration scheme. Problems due to the singularity in the equations of motion at the pole have been eliminated by using a rotated spherical coordinate system at each grid point poleward of a certain latitude. The model contained no diffusion, other than the inherent numerical diffusion of the semi-Lagrangian scheme, and no polar filtering was employed. Divergence damping was included as an option, but was not always needed. Starting from a geostrophically balanced initial state of planetary scale, it was found possible to carry out accurate integrations for a 5-day pe-

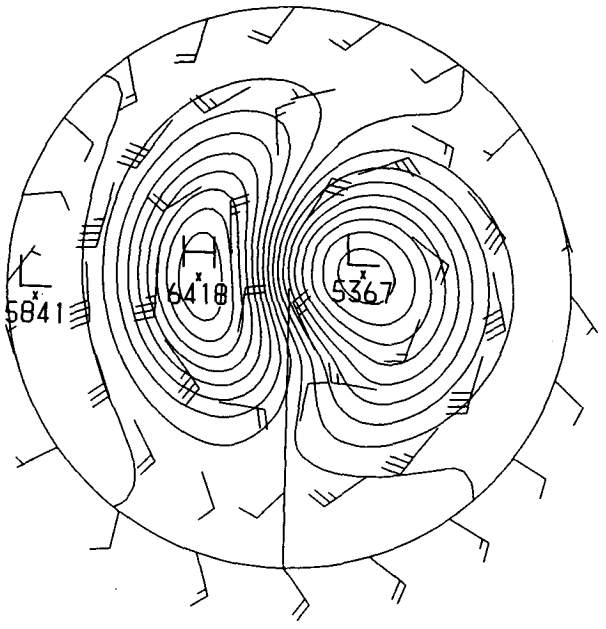

FIG. 6. Integration at day 5 with Δt = 1 h, c = 0 (remaining parameters as in Fig. 4).

riod, even without divergence damping, using a time step of 1 h.

Acknowledgments. We are grateful to our colleagues, Drs. Jim Hamilton and Peter Lynch at the Irish Meteorological Service, and Fredrick Semazzi at the NASA Goddard Laboratory for Atmospheres, for useful discussions and for help in carrying out this work. J. R. Bates wishes to acknowledge support through NASA Grant NAG-867 to the University of Maryland.

APPENDIX A

Transformation Formulae for the Auxiliary Spherical Coordinate System

Consider an arbitrary point P on the surface of the earth whose coordinates in the geographical spherical system are (λ, θ). We wish to calculate its coordinates (λ', θ') in the auxiliary spherical coordinate system defined at point A, where $(\lambda, \theta) = (\lambda_I, \theta_J)$, $(\lambda', \theta') = (0, 0)$, and the unit vectors $(\mathbf{i}, \mathbf{j})$ in both systems coincide (see Fig. 2).

We find the required transformation formulae by making use of associated Cartesian coordinate systems whose origins lie at C, the center of the earth. Associated with the geographical system (λ, θ) we define a Cartesian system having unit vectors $(\mathbf{I}, \mathbf{J}, \mathbf{K})$; $\mathbf{I}$ lies along the line connecting C to the point where $(\lambda, \theta) = (0, 0)$, $\mathbf{J}$ lies along the line connecting C to the point where $(\lambda, \theta) = (\pi/2, 0)$ and $\mathbf{K}$ points along the earth's axis towards the north pole. The corresponding Cartesian system associated with the auxiliary spherical system at point A is obtained by performing two rotations; in the first, the system $(\mathbf{I}, \mathbf{J}, \mathbf{K})$ is rotated through the angle λ_I about $\mathbf{K}$, giving an intermediate system $(\hat{\mathbf{I}}, \hat{\mathbf{J}}, \hat{\mathbf{K}})$; in the second the intermediate system is rotated through the angle $-\theta_J$ about $\hat{\mathbf{J}}$, giving the new system $(\mathbf{I}', \mathbf{J}', \mathbf{K}')$.

The Cartesian coordinates of P are related to its coordinates in the associated spherical system by the formulae

$$x = a\cos\theta\cos\lambda \tag{A1}$$

$$y = a\cos\theta\sin\lambda \tag{A2}$$

$$z = a\sin\theta. \tag{A3}$$

Applying these formulae to the intermediate system and using the fact that the coordinates of P in this system are defined by $(\hat{\lambda}, \hat{\theta}) = (\lambda - \lambda_I, \theta)$ we have

$$\hat{x} = a\cos\theta\cos(\lambda - \lambda_I) \tag{A4}$$

$$\hat{y} = a\cos\theta\sin(\lambda - \lambda_I) \tag{A5}$$

$$\hat{z} = a\sin\theta. \tag{A6}$$

The second rotation takes place in the $(\hat{x}, \hat{z})$ plane and immediately gives

$$x' = \hat{x}\cos\theta_J + \hat{z}\sin\theta_J \tag{A7}$$

$$y' = \hat{y} \tag{A8}$$

$$z' = \hat{z}\cos\theta_J - \hat{x}\sin\theta_J \tag{A9}$$

where (x', y', z') are the Cartesian coordinates of P in the system $(\mathbf{I}', \mathbf{J}', \mathbf{K}')$. Eliminating $(\hat{x}, \hat{y}, \hat{z})$ from (A7)–(A9) using (A4), (A5), (A6) we have

$$x' = a[\cos\theta\cos(\lambda - \lambda_I)\cos\theta_J + \sin\theta\sin\theta_J] \tag{A10}$$

$$y' = a[\cos\theta\sin(\lambda - \lambda_I)] \tag{A11}$$

$$z' = a[\sin\theta\cos\theta_J - \cos\theta\cos(\lambda - \lambda_I)\sin\theta_J]. \tag{A12}$$

But (x', y', z') are related to (λ', θ') by formulae identical in form to (A1), (A2), (A3). Equating these formulae to (A10), (A11), (A12) we arrive at (19, 20, 21).

To obtain the formula (24) relating the velocity components in the two coordinate systems, we take the total derivatives of (19), (20), (21), giving

$$u'\sin\lambda' + v'\sin\theta'\cos\lambda' = u\sin(\lambda - \lambda_I)\cos\theta_J + v[\sin\theta\cos(\lambda - \lambda_I)\cos\theta_J - \cos\theta\sin\theta_J] \tag{A13}$$

$$u'\cos\lambda' - v'\sin\theta'\sin\lambda' = u\cos(\lambda - \lambda_I) - v\sin\theta\sin(\lambda - \lambda_I) \tag{A14}$$

$$v'\cos\theta' = u\sin(\lambda - \lambda_I)\sin\theta_J + v[\cos\theta\cos\theta_J + \sin\theta\cos(\lambda - \lambda_I)\sin\theta_J]. \tag{A15}$$

Taking [(A13) × sinλ′ + (A14) × cosλ′] we have

$$u' = \sin\lambda'[u\sin(\lambda - \lambda_I)\cos\theta_J + v\{\sin\theta\cos(\lambda - \lambda_I)\cos\theta_J - \cos\theta\sin\theta_J\}] + \cos\lambda'[u\cos(\lambda - \lambda_I) - v\{\sin\theta\sin(\lambda - \lambda_I)\}].$$

Eliminating $(\cos\lambda', \sin\lambda')$ from this equation using (19, 20), we arrive at the expression for u' in (24).

The expression for v' in (24) follows immediately from (A15).

APPENDIX B

Determination of the Departure Points for the Poles

We first consider the north pole. If the vector wind is constant in the immediate neighborhood of the pole, its components can be written at any point within this neighborhood as

$$u_p = V_p\sin(\lambda - \lambda_0) \tag{B1}$$

$$v_p = V_p\cos(\lambda - \lambda_0) \tag{B2}$$

where V_p is the magnitude of the wind vector and λ_0 is the longitude from which it blows toward the pole.

We identify (B2) with the first Fourier component of $v^{n+1/2}[\lambda_i, (\pi/2) - (\Delta\theta/2)]$, the time-centered es-

timated of v at the nearest v-points to the pole. Hence we find

$$V_p = (a^2 + b^2)^{1/2}$$

$$\lambda_0 = \tan^{-1}(b/a)$$

where

$$a = \frac{2}{N}\sum_{i=1}^{N} v^{n+1/2}\left(\lambda_i, \frac{\pi}{2} - \frac{\Delta\theta}{2}\right)\cos\lambda_i$$

$$b = \frac{2}{N}\sum_{i=1}^{N} v^{n+1/2}\left(\lambda_i, \frac{\pi}{2} - \frac{\Delta\theta}{2}\right)\sin\lambda_i$$

N being the number of gridpoints on a latitude circle.

The departure point for the North Pole corresponding to the time interval Δt is then given by

$$\lambda_* = \tan^{-1}(b/a) \tag{B3}$$

$$\theta_* = \frac{\pi}{2} - \frac{V_p \Delta t}{a}. \tag{B4}$$

Applying similar considerations to the south pole, we find that the departure point is given by

$$\lambda_* = \pi + \tan^{-1}(b/a) \tag{B5}$$

$$\theta_* = -\frac{\pi}{2} + \frac{V_p \Delta t}{a} \tag{B6}$$

where (a, b, V_p) are evaluated as above, using the time-centered estimates of v at the nearest v-points to the south pole.

REFERENCES

Bates, J. R., 1984: An efficient semi-Lagrangian and alternating direction implicit method for integrating the shallow water equations. *Mon. Wea. Rev.*, **112**, 2033–2047.

——, and A. McDonald, 1982: Multiply-upstream, semi-Lagrangian advective schemes: Analysis and application to a multilevel primitive equation model. *Mon. Wea. Rev.*, **110**, 1831–1842.

——, and ——, 1987: A semi-Lagrangian and alternating direction implicit method for integrating a multilevel primitive equation model. *Short and Medium-Range Numerical Weather Prediction*, Papers presented at the WMO/IUGG NWP Symp., Tokyo, 1986, Meteor. Soc. Japan, 223–232.

Coté, J., and A. Staniforth, 1988: A two-time-level semi-Lagrangian semi-implicit scheme for spectral models. *Mon. Wea. Rev.*, **116**, 2003–2012.

McDonald, A., 1986: A semi-Lagrangian and semi-implicit two time-level integration scheme. *Mon. Wea. Rev.*, **114**, 824–830.

——, and J. R. Bates, 1987: Improving the estimate of the departure point position in a two-time level semi-Lagrangian and semi-implicit scheme. *Mon. Wea. Rev.*, **115**, 737–739.

Ritchie, H., 1988: Application of the semi-Lagrangian method to a spectral model of the shallow water equations. *Mon. Wea. Rev.*, **116**(8), 1587–1598.

Robert, A., 1981: A stable numerical integration scheme for the primitive meteorological equations. *Atmos.-Ocean*, **19**, 35–46.

——, 1982: A semi-Lagrangian and semi-implicit numerical integration scheme for the primitive meteorological equations. *J. Meteor. Soc. Japan*, **60**, 319–324.

——, T. L. Yee and H. Ritchie, 1985: A semi-Lagrangian and semi-implicit integration scheme for multi-level atmospheric models. *Mon. Wea. Rev.*, **113**, 388–394.

Staniforth, A. N., and C. Temperton, 1986: Semi-implicit semi-Lagrangian integration schemes for a barotropic finite-element regional model. *Mon. Wea. Rev.*, **114**, 2078–2090.

Sweet, R. A., 1977: A cyclic reduction algorithm for solving block tridiagonal systems of arbitrary dimension. *SIAM J. Numer. Anal.*, **14**, 706–720.

Temperton, C., and A. N. Staniforth, 1987: An efficient two-time-level semi-Lagrangian semi-implicit integration scheme. *Quart. J. Roy. Meteor. Soc.*, **113**, 1025–1039.